Efficient green emission from (11(2)over-bar2) InGaN/GaN quantum wells on GaN microfacets probed by scanning near field optical microscopy

AUTHOR(S):

Kawakami, Y; Nishizuka, K; Yamada, D; Kaneta, A; Funato, M; Narukawa, Y; Mukai, T

CITATION:

Kawakami, Y ...[et al]. Efficient green emission from (11(2)over-bar2) InGaN/GaN quantum wells on GaN microfacets probed by scanning near field optical microscopy. APPLIED PHYSICS LETTERS 2007, 90(26): 261912.

ISSUE DATE:

2007-06-25

URL:

http://hdl.handle.net/2433/50152

APPLIED PHYSICS LETTERS **90**, 261912 (2007)

Efficient green emission from (11$\bar{2}$2) InGaN/GaN quantum wells on GaN microfacets probed by scanning near field optical microscopy

Y. Kawakami,[a] K. Nishizuka, D. Yamada, A. Kaneta, and M. Funato
Department of Electronic Science and Engineering, Kyoto University, Kyoto 615-8510, Japan

Y. Narukawa and T. Mukai
Nitride Semiconductor Research Laboratory, Nichia Corporation, Tokushima 774-8601, Japan

(Received 29 March 2007; accepted 18 May 2007; published online 28 June 2007)

Nanoscopic optical characterization using scanning near field optical microscopy was performed on a (11$\bar{2}$2) microfacet quantum well (QW). It was revealed that the carrier diffusion length in the (11$\bar{2}$2) QW is less than the probing fiber aperture of 160 nm, which is shorter than that of the (0001) QWs and is attributed to much faster radiative recombination processes in the (11$\bar{2}$2) QW due to a reduced internal electric field. Owing to this short diffusion length, the correlation between the internal quantum efficiency (IQE) and emission wavelength is elucidated. The highest IQE is ~50% at 520 nm, which is about 50 nm longer than in (0001) QWs, suggesting that the (11$\bar{2}$2) QW is a suitable green emitter. © *2007 American Institute of Physics*. [DOI: 10.1063/1.2748309]

InGaN-based quantum wells (QWs) in semipolar and nonpolar directions have received increased attention due to their potential high emission efficiency caused by reduced or negligible polarization effects.[1–8] We recently demonstrated that {11$\bar{2}$2} semipolar planes are promising for low internal electric fields when these planes naturally appear as microfacets through the regrowth process on *c*-oriented GaN templates.[2,3] This finding has motivated fabrication of InGaN/GaN light-emitting diodes (LEDs) on GaN {11$\bar{2}$2},[4] (1$\bar{1}$00),[6,7] and (1$\bar{1}$01) substrates.[8] The device performances are already suitable for practical applications and have recently been catching up to those in conventional (0001) InGaN/GaN LEDs.[7,8] However, a comprehensive understanding of the optical properties will be indispensable to draw higher device performances.

In (0001) InGaN QWs, it has been reported that carrier/exciton localization in potential minima plays a crucial role in determining the optical properties.[9,10] The dimension of potential fluctuations is on the order of nanometers, and therefore, nanospectroscopy using scanning near field microscopy (SNOM) is a powerful tool to assess the optical properties derived from carrier localization phenomena. We have developed a SNOM system for InGaN QWs and have revealed the temporal and spatial carrier dynamics.[11,12] In particular, comparing images obtained from the illumination-collection (*I-C*) mode, which uses an identical fiber to excite and detect photoluminescence (PL), and those from the illumination (*I*) mode, which detects PL excited through a fiber in a far field, has provided insight into radiative recombination, nonradiative recombination, and diffusion processes.[12] In this study, we applied SNOM to a (11$\bar{2}$2) microfacet QW. It is found that the carriers in a (11$\bar{2}$2) QW are less diffusive than those in (0001) QWs, and unlike those of (0001) QWs, the internal quantum efficiency (IQE) of the (11$\bar{2}$2) QW is the highest in the green spectral range.

The sample studied here is the same InGaN/GaN microfacet single QW as that in Ref. 4, consisted of semipolar {11$\bar{2}$2} microfacets as well as (0001) and {11$\bar{2}$0} facets, as shown in Fig. 1(a). The thicknesses of the InGaN well and GaN cap on the {11$\bar{2}$2} facets were 2 and 20 nm, respectively. The InGaN well width was rather uniform (2.0±0.2 nm) within the {11$\bar{2}$2} facet, but the In composition estimated by energy dispersive x-ray spectroscopy monotonously increased from 25% on the {11$\bar{2}$0} side to 40% on the (0001) side. This large intrafacet variation of the In composition led to a broad emission; the PL spectrum acquired at room temperature (RT) peaked at 535 nm (2.32 eV) and encompassed wavelengths from 450 to 650 nm. From the temperature dependence of the integrated PL intensity, the IQE averaged over the entire spectral range was as high as 33% at RT, despite including a red component. To determine the cause of the observed high IQE, time-resolved PL measurements were performed and the radiative lifetimes were estimated to be 72 ps at 460 nm (blue), 161 ps at 530 nm (green), and 181 ps at 575 nm (amber) at low temperatures.

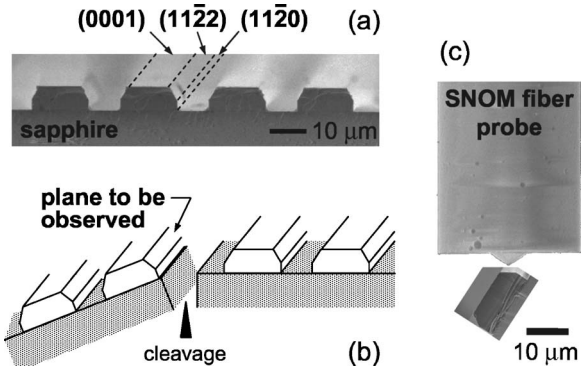

FIG. 1. (a) Cross sectional Scanning electron microscopy (SEM) image of microfacet structures composed of (0001), {11$\bar{2}$2}, and {11$\bar{2}$0} facets. (b) Cleavage of the sample for SNOM observations of a (11$\bar{2}$2) microfacet QW. (c) SEM images of the fiber probe for SNOM and the sample showing how the fiber approaches the sample.

[a]Electronic mail: kawakami@kuee.kyoto-u.ac.jp

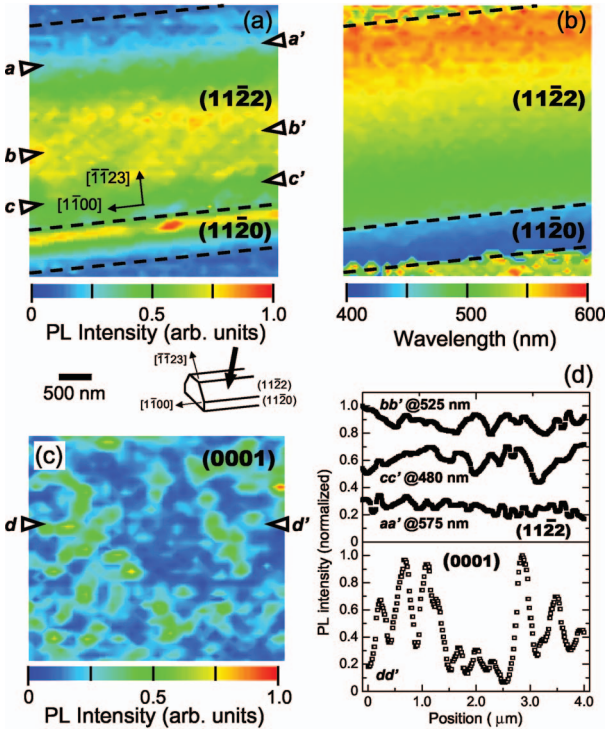

FIG. 2. (Color) (a) PL peak intensity and (b) wavelength mapping of the (11$\bar{2}$2) microfacet QW acquired at RT. (c) RT-PL intensity mapping of a conventional planar (0001) InGaN/GaN QW on ELO-GaN. (d) Intensity variations along *aa'*, *bb'*, and *cc'* in the (11$\bar{2}$2) QW and *dd'* in the (0001) QW.

Furthermore, the estimated radiative lifetime at 530 nm at RT was 400 ps. Typically, the radiative lifetimes in 3-nm-thick (0001) QWs are 15 ns at 450 nm, 85 ns at 520 nm, and 1 μs at 630 nm at low temperatures. Thus, it is clear that the {11$\bar{2}$2} QW possesses a much shorter and smaller wavelength dependent radiative lifetimes, which is well accounted for by the weaker polarization effects in the {11$\bar{2}$2} QWs. As discussed below, such short lifetimes affect the spatial carrier dynamics.

SNOM observations were performed at RT using a fiber probe, which had a single-tapered pure SiO_2 core with an aperture diameter of 160 nm. The excitation source was a frequency doubled Ti:sapphire laser, which emitted at 380 nm to selectively excite the InGaN well. Due to the limitation that arises from the dimensions of the fiber probe and the microstructures, the sample for SNOM observations was prepared as schematically illustrated in Fig. 1. The excitation power density ranged from 1.6 to 160 $\mu J/cm^2$, which corresponds to a photogenerated carrier density from $\sim 1 \times 10^{17}$ to $\sim 1 \times 10^{19}/cm^3$, but a clear dependence on the excitation power was not detected in the PL spectra. PL was introduced into a 50 cm monochromator and was detected by a liquid-nitrogen-cooled charge coupled device detector.

Figure 2 shows the spatial distributions of (a) the PL peak intensity and (b) the peak wavelength in the (11$\bar{2}$2) microfacet QW acquired under the *I-C* mode at RT. The PL intensity drastically varied perpendicular to the facet boundary ($\parallel$[$\bar{1}\bar{1}$23]), while the PL intensity remained nearly unchanged along the facet boundary ($\parallel$[1$\bar{1}$00]). Similarly, the PL peak wavelength exhibited large variations only along the [$\bar{1}\bar{1}$23] direction [Fig. 2(b)], which suggests a strong correlation between the PL intensity and wavelength, as discussed below. The PL peak wavelength was 476 nm (2.6 eV) on the (11$\bar{2}$0) side of the (11$\bar{2}$2) facet and monotonously increased to 590 nm (2.1 eV) on the (0001) side due to the above-mentioned spatial distribution for the In composition.

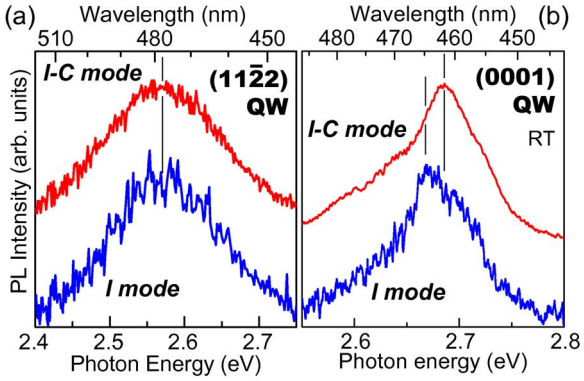

FIG. 3. (Color online) PL spectra taken at RT under the *I-C* and *I* modes for 2(a) the (11$\bar{2}$2) and (b) (0001) QWs.

The inhomogeneity of the PL intensity observed in Fig. 2(a) indicates that the (11$\bar{2}$2) microfacet QW involves potential fluctuations on the order of 100 nm or less. On the other hand, Fig. 2(c) shows the PL intensity mapping of a planar (0001) InGaN/GaN QW fabricated on epitaxially laterally overgrown (ELO) GaN. This QW emits at 520 nm and the PL intensity mapping was obtained under the same experimental conditions. Although the size of the islandlike structures, that is, the intensity fluctuations, appears similar, the degree of intensity variation drastically differs, as summarized in Fig. 2(d), which compares the line scans of the normalized PL intensities along *aa'*, *bb'*, and *cc'* in the (11$\bar{2}$2) QW and along *dd'* in the (0001) QW. The line scans *aa'*, *bb'*, and *cc'* are aligned in the [1$\bar{1}$00] direction and, therefore, correspond to PL intensity variations at emission wavelengths of 575, 525, and 480 nm, respectively. As can be seen in Fig. 2(d), the line scans vary by only 20%, whereas the PL intensity in the (0001) QW is largely scattered about 80%. In order to elucidate the reason for this striking difference, SNOM was performed under the *I* mode for both the QWs.

Figures 3(a) and 3(b) show examples of the PL spectra for the (11$\bar{2}$2) microfacet QW and (0001) QW, respectively, acquired at RT by the *I-C* and *I* modes. The PL measurements by the *I-C* and *I* modes were performed at the same position. For the (0001) QW [Fig. 3(b)], the PL under the *I-C* mode is located at a higher energy, suggesting that the position beneath the fiber probe has a higher potential and the photogenerated carriers diffuse outside the fiber aperture. After diffusion, the carriers experience a lower potential and emit at lower energy, as observed in the *I* mode. On the other hand, for the (11$\bar{2}$2) QW, the PL spectra obtained by the *I-C* and *I* modes are always identical, as shown in typical PL spectra in Fig. 3(a). This observation indicates that carrier diffusion toward outside the fiber probe is absent.

The carrier diffusion length λ is described by the equation of $\lambda = \sqrt{D\tau}$, where D is the diffusion coefficient and τ is the carrier lifetime. The diffusion coefficient for the {11$\bar{2}$2} plane is unknown, but currently we believe that τ is respon-

sible for a shorter diffusion length in the $(11\bar{2}2)$ QW. The PL lifetimes at RT were measured to be ~200 ps for the $(11\bar{2}2)$ QW and 40 ns for a conventional (0001) QW emitting at 520 nm. The much shorter PL lifetime for the $(11\bar{2}2)$ QW is mainly due to the considerably shorter radiative lifetime of 400 ps at RT. Because the PL lifetime corresponds to the carrier lifetime τ, the difference of two orders of magnitude in the PL lifetimes (i.e., carrier lifetimes) results in one order of difference in the diffusion length, assuming equivalent diffusion coefficients for the $\{11\bar{2}2\}$ and (0001) planes. The diffusion length in (0001) InGaN QWs (In: 8%–25%) has been reported to range from 200 to 600 nm.[12,13] Therefore, the diffusion length in the $(11\bar{2}2)$ InGaN/GaN QW can be as low as 20–60 nm, which is smaller than the 160 nm fiber aperture. Thus, it is reasonable that diffusion is absent according to the present SNOM system because the recombination processes in the $(11\bar{2}2)$ QW are completed within the fiber aperture.

Let us discuss the cause of the difference in PL intensity variations observed between the $(11\bar{2}2)$ and reference (0001) QWs [Fig. 2(d)]. Because both the QWs were fabricated with similar regrowth techniques, the properties related to threading dislocations, which work as the nonradiative recombination centers (NRCs), should not differ significantly. In addition, the degree of potential fluctuations appears to be comparable because the PL linewidths measured by SNOM were equivalent. Thus, these factors can be excluded from the current discussion and at present, we attribute the uniform PL intensity distribution for the $(11\bar{2}2)$ QW to the short diffusion length. For (0001) QWs, the fiber aperture and the diffusion length are comparable. Therefore, NRCs located in the vicinity of the fiber probe capture almost all carriers generated within the fiber aperture, which produces weak PL and generates a striking contrast with PL obtained away from NRCs. On the other hand, for the $(11\bar{2}2)$ QW, even when the fiber aperture includes NRCs, only a part of carriers are captured by the NRCs due to the short diffusion length. Consequently, NRCs do not affect the PL intensity seriously, which makes PL intensity mapping uniform.

The *I*-*C* and *I* modes provide identical images for the $(11\bar{2}2)$ QW, while the PL intensity measured by the *I* mode is proportional to the local IQE, in principle.[12] Therefore, the PL intensity mapping in Fig. 2(a) represents a spatial distribution of the IQE in the $(11\bar{2}2)$ QW and Figs. 2(a) and 2(b) can be used to reveal the correlation between the IQE and the emission wavelength. The result is shown in Fig. 4 where the IQE was evaluated so that an average macroscopic IQE of 33% is reproduced. For comparison, the IQEs of reference (0001) QWs are also plotted. The trend of the (0001) QWs is typical and the IQE is the highest around 460 nm when a technique is not used to reduce threading dislocations, that is, blue LEDs emit much more efficiently than green LEDs. On the other hand, the IQE in the $(11\bar{2}2)$ QW reaches a maximum of 50% at a longer wavelength of 520 nm, which strongly suggests that the $(11\bar{2}2)$ QWs are suitable for green emitters.

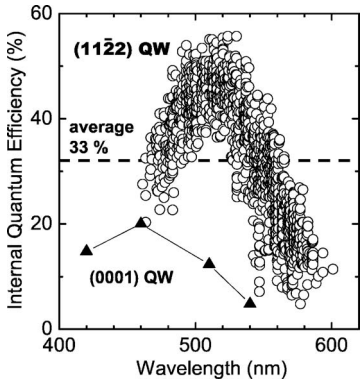

FIG. 4. IQE as a function of the emission wavelength, which is extracted from Figs. 2(a) and 2(b). Those for conventional (0001) QWs are plotted for comparison.

Finally, the dimensions of the radiative recombination centers (RRCs) are discussed. Each PL spectrum taken by SNOM had a linewidth of ~180 meV irrespectively of the measurement position, within which the contribution from the In composition gradient along the $[\bar{1}\bar{1}23]$ direction is ~30 meV. Therefore, many RRCs should exist within the aperture. In fact, analyses of the radiative recombination lifetimes based on a modified quantum disk model[14] suggest that the diameter of RRCs is 15–20 nm, which is consistent with the SNOM observation. Considering Fig. 2(a), it is concluded that the $(11\bar{2}2)$ QW involves potential fluctuations of about 20 nm, which work as RRCs and overlap with spatially larger potential fluctuations on the order of 100 nm.

[1] P. Waltereit, O. Brandt, A. Trampert, H. T. Grahn, J. Menniger, M. Ramsteiner, M. Reiche, and K. H. Ploog, Nature (London) **406**, 865 (2000).
[2] K. Nishizuka, M. Funato, Y. Kawakami, Sg. Fujita, Y. Narukawa, and T. Mukai, Appl. Phys. Lett. **85**, 3122 (2004).
[3] K. Nishizuka, M. Funato, Y. Kawakami, Y. Narukawa, and T. Mukai, Appl. Phys. Lett. **87**, 231901 (2005).
[4] M. Funato, M. Ueda, Y. Kawakami, Y. Narukawa, T. Kosugi, M. Takahashi, and T. Mukai, Jpn. J. Appl. Phys., Part 2 **45**, L659 (2006).
[5] M. Ueda, K. Kojima, M. Funato, Y. Kawakami, Y. Narukawa, and T. Mukai, Appl. Phys. Lett. **89**, 211907 (2006).
[6] K. Okamoto, H. Ohta, D. Nakagawa, M. Sonobe, J. Ichihara, and H. Takasu, Jpn. J. Appl. Phys., Part 2 **45**, L1197 (2006).
[7] M. C. Schimidt, K.-C. Kim, H. Sato, N. Fellows, H. Masui, S. Nakamura, S. P. DenBaars, and J. S. Speck, Jpn. J. Appl. Phys., Part 2 **46**, L126 (2007).
[8] A. Tyagi, H. Zhong, N. N. Fellows, M. Iza, J. S. Speck, S. P. DenBaars, and S. Nakamura, Jpn. J. Appl. Phys., Part 2 **46**, L129 (2007).
[9] S. Chichibu, T. Azuhatra, T. Sota, and S. Nakamura, Appl. Phys. Lett. **69**, 4188 (1996).
[10] Y. Narukawa, Y. Kawakami, M. Funato, Sz. Fujita, Sg. Fujita, and S. Nakamura, Appl. Phys. Lett. **70**, 981 (1997).
[11] A. Kaneta, G. Marutsuki, Y. Narukawa, T. Mukai, K. Okamoto, Y. Kawakami, and Sg. Fujita, Appl. Phys. Lett. **81**, 4353 (2002).
[12] A. Kaneta, T. Mutoh, G. Marutsuki, Y. Narukawa, T. Mukai, Y. Kawakami, and Sg. Fujita, Appl. Phys. Lett. **83**, 3462 (2003).
[13] S. J. Rosner, G. Girolami, H. Marchand, P. T. Fini, J. P. Ibbetson, L. Zhao, S. Keller, U. K. Mishra, S. P. DenBaars, and J. S. Speck, Appl. Phys. Lett. **74**, 2035 (1999).
[14] M. Funato, Y. Kawaguchi, and Sg. Fujita, Mat. Res. Soc. Symp. Proc., **798**, 347 (2004).